Accepted Manuscript

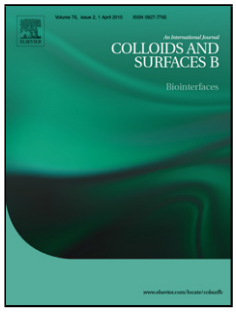

Title: Lipid selectivity in novel antimicrobial peptides: implication on antimicrobial and hemolytic activity

Authors: P. Maturana, M. Martinez, M. Noguera, N.C. Santos, E.A. Disalvo, L. Semorile, P.C. Maffia, A. Hollmann

PII: S0927-7765(17)30075-9
DOI: http://dx.doi.org/doi:10.1016/j.colsurfb.2017.02.003
Reference: COLSUB 8375

To appear in: *Colloids and Surfaces B: Biointerfaces*

Received date: 2-8-2016
Revised date: 10-1-2017
Accepted date: 4-2-2017

Please cite this article as: P.Maturana, M.Martinez, M.Noguera, N.C.Santos, E.A.Disalvo, L.Semorile, P.C.Maffia, A.Hollmann, Lipid selectivity in novel antimicrobial peptides: implication on antimicrobial and hemolytic activity, Colloids and Surfaces B: Biointerfaces http://dx.doi.org/10.1016/j.colsurfb.2017.02.003

Lipid selectivity in novel antimicrobial peptides: implication on antimicrobial and hemolytic activity

Maturana, P.[1];Martinez, M.[2]; Noguera M. [3]; Santos, N.C.[4] ; Disalvo, E. A.[1]; Semorile, L.[2], Maffia P.C.[2*±]; Hollmann, A.[1,2*±]

[1]Laboratory of Biointerfaces and Biomimetic Systems- CITSE – National University of Santiago del Estero, Santiago del Estero and CONICET, Argentina.

[2]Laboratory of Molecular Microbiology, Institute of Basic and Applied Microbiology, University of Quilmes, B1876BXD Bernal, Argentina.

[3]Instituto de Química y Fisicoquímica Biológicas, CONICET-University of Buenos Aires, Buenos Aires, Argentina

[4]Instituto de Medicina Molecular, Faculdade de Medicina, Universidade de Lisboa, Lisbon, Portugal.

Statistical summary of the article: Number of words: 6045

Tables/figures: 7

± Equal contributors, shared senior authorship of the paper

*Corresponding authors: ahollmann@unq.edu.ar (A.Hollmann);

paulo.maffia@unq.edu.ar (P.C. Maffía).

Graphical Abstract

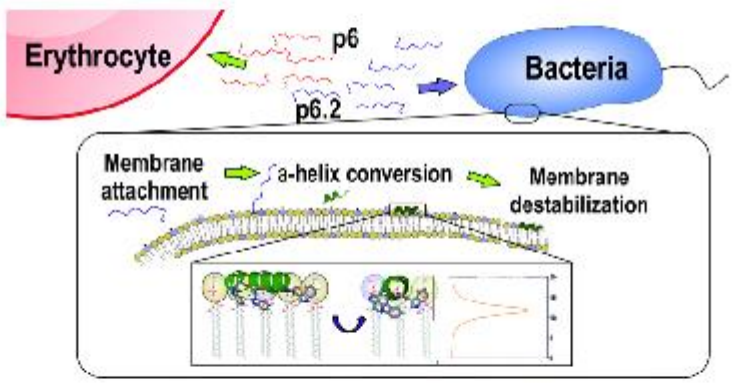

Highlights:

- Selectivity of the peptides for zwitterionic or negatively charged lipids determine its bioactivity
- Affinity toward negatively lipid instead zwitterionics drives from hemolytic to antimicrobial results
- α-helix structure of p6.2 increases its ability to interact with negatively charged membranes

ABSTRACT

Antimicrobial peptides (AMPs) are small cationic molecules that display antimicrobial activity against a wide range of bacteria, fungi and viruses. For an AMP to be considered as a therapeutic option, it must have not only potent antibacterial properties but also low hemolytic and cytotoxic activities [1]. Even though many studies have been conducted in order to correlate the antimicrobial activity with affinity toward model lipid membranes, the use of these membranes to explain cytotoxic effects (especially hemolysis) has been less explored. In this context, we studied lipid selectivity in two related novel AMPs, peptide 6 (P6) and peptide 6.2 (P6.2). Each peptide was designed from a previously reported AMP, and specific amino acid

replacements were performed in an attempt to shift their hydrophobic moment or net charge. P6 showed no antimicrobial activity and high hemolytic activity, and P6.2 exhibited good antibacterial and low hemolytic activity. Using both peptides as a model we correlated the affinity toward membranes of different lipid composition and the antimicrobial and hemolytic activities. Our results from surface pressure and zeta potential assays showed that P6.2 exhibited a higher affinity and faster binding kinetic toward PG-containing membranes, while P6 showed this behavior for pure PC membranes. The final position and structure of P6.2 into the membrane showed an alpha-helix conversion, resulting in a parallel alignment with the Trp inserted into the membrane. On the other hand, the inability of P6 to adopt an amphipathic structure, plus its lower affinity toward PG-containing membranes seem to explain its poor antimicrobial activity. Regarding erythrocyte interactions, P6 showed the highest affinity toward erythrocyte membranes, resulting in an increased hemolytic activity. Overall, our data led us to conclude that affinity toward negatively charged lipids instead of zwitterionic ones seems to be a key factor that drives from hemolytic to antimicrobial activity.

Keywords: Antimicrobial peptides; Membrane affinity; Hemolysis;

INTRODUCTION

Antimicrobial peptides (AMPs) are a key factor in the innate immunity, which serves as the first line of defense against bacterial and fungal infections in a wide range of hosts, from plants to humans [2]. The efficiency of AMPs is attributed to their ability to disrupt the cellular membranes of microorganisms, in some cases causing pore generation, thus leading to microbial death [3]. Binding of cationic AMPs to a bacterial

membrane is driven by electrostatic contacts between the positively charged amino acids and the negatively charged cell surface, followed by hydrophobic interactions between the amphipathic domains of the peptide and the membrane phospholipids. The mechanism of action of these peptides leaves the target organism less able to adapt or develop resistance toward AMPs [4]. As a result, these molecules typically have a wide spectrum of antimicrobial activity, which makes AMPs very important resources for human therapeutics as lead compounds to counteract the current drug resistance development [5]. Despite their variations, the key features that render them to exhibit microbicidal activity are i) their cationicity, ii) their binding to bacterial membranes and iii) the adoption of secondary structure in membrane environments [6]. These characteristics allow them to attach to and insert into the bacterial membrane rather than host membranes. Most AMPs are thought to target the bacterial plasma membrane directly rather than through specific protein receptors [7]. Therefore the phospholipid composition, in particular the net charge of the membranes plays a key role in determining the antimicrobial activity of the AMPs [8]. Despite their microbial membrane affinity, amphipathic cationic antimicrobial peptides (CAMPs) can also interact and disassemble the membrane of eukaryotic cells, particularly erythrocytes. The eukaryotic cell selectivity is a possible undesirable feature of CAMPs, which represent a challenge to be addressed when designing new CAMPs sequences. In this context, AMP's selectivity is often measured by the so-called therapeutic index, defined as the ratio between their minimum hemolytic concentration (MHC) and minimum inhibitory concentrations (MIC): MHC/MIC [9, 10]. The higher the therapeutic index (MHC/MIC), the more effective the AMP would be as an antibiotic. Accordingly, there have been many attempts to clarify the parameters that control the selectivity of AMPs.[10-12].

Model membrane systems, such as lipid vesicles, have been used for three decades to explore the structure, function, and mechanism of AMPs [13, 14]. Despite the huge contribution from the scientific community in this field, the focus has generally been set in predicting and unravels their antimicrobial effects, while a proper insight on the cytotoxic or the hemolytic activity of AMPs has been less studied. In this work we have designed and characterize two cationic peptides: P6 and P6.2. Both peptides were designed from a previously reported antimicrobial peptide (Seq2) [15], whose backbone was used as a scaffold to design the two new sequences. Specific amino acid substitutions were made in order to shift the hydrophobicity and hydrophobic moment of the parent peptide Seq2. The first round of substitutions introduced rendered a sequence with high hemolytic values and poor antimicrobial activity (P6), while subsequent substitutions produced a peptide (P6.2) with lower hemolytic activity and a dramatic increase in antimicrobial activity.

With these two related sequences, we studied in detail the interaction of the peptides in simple membrane mimetic models in order to establish the lipid selectivity of each peptide, in other words, the preferential interaction for a zwiterionic membrane or a negatively charged one. For this approach we used large unilamellar vesicles (LUVs) and lipid monolayers, using the phospholipid dimyristoyl phosphatidylcholine (DMPC) with zwitterionic head groups (i.e. without a net charge) and dimyristoyl phosphatidylglycerol (DMPG) with anionic head groups. Finally, to correlate these findings, we evaluated the affinity of both peptides with erythrocyte membranes.

MATERIAL AND METHODS

Peptide synthesis

Each peptide was synthesized with C terminus amidation. Peptides were synthesized and obtained at a purity grade of >95% by HPLC (GenScript Co., Piscataway, NJ 08854, USA). The peptide sequences were: peptide 6: GLLWKWGWKWKEFLRIVGY and peptide 6.2: GLLRKWGKKWKEFLRRVWK.

Analysis of physicochemical properties

For the analysis of net charge, hydrophobic moment, hydrophobicity, isoelectric point and molecular weight, we used the online programs Heliquest [16] (http://heliquest.ipmc.cnrs.fr/cgi-bin/ComputParamsV2.py), and Agadir (http://agadir.crg.es/) [17]. The mean hydrophobicity (H) and the mean hydrophobic moment (μH) were calculated from the amino acid sequences, using the Eisenberg scale for hydrophobicity by the HydroMCalc applet [10] and Heliquest. The helical wheel projections diagrams were obtained from Heliquest.

Antimicrobial activity

Minimal inhibitory concentration (MIC) was determined by standard microdilution assay according to CLSI recommendations [13], using Mueller Hinton Broth (DIFCO) supplemented with Ca^{2+} (20-25mg/L) and Mg^{2+} (10-12.5mg/L). The bacterial strains used were *Pseudomonas aeruginosa* ATCC® 47085 and *Staphylococcus aureus* ATCC® 25923

Hemolytic assay

The hemolytic activity of the peptides was evaluated according to the method described

previously [18]. Briefly, a volume of heparinized human whole blood was diluted 1:3 in phosphate-buffered saline and then centrifuged 10 min. at 1500 rpm. This procedure was repeated three more times. The cell pellet was resuspended in phosphate-buffered saline to a final dilution of 0.5% (*v/v*). Peptides were then added at different concentrations and incubated at 37 ºC for 30 min. Afterwards, tubes were centrifuged and the absorbance of the supernatant at 550 nm was measured. The percentage lysis was then calculated relative to 0% lysis with buffer and 100% lysis with water. The absorbance measurement was repeated three times, and the averaged values were used.

Aggregation assay

A solution containing 25.6 μM of 8-Anilino-1-naphthalenesulfonic acid ammonium salt (1-8-ANS, Sigma Aldrich, GmbH, Germany) in HEPES buffer was titrated with a stock solution of each peptide to achieve a final concentration within the range of 0-24 μM. ANS fluorescence emission measurements were recorded from 400 nm to 650 nm with a λexc = 369 nm. Incubation temperature was set at 20 °C.

Lipids

The zwitterionic lipid DMPC (1,2-dimyristoyl-sn-glycero-3-phosphocholine) and negatively charged lipid DMPG (1,2-dimyristoyl-sn-glycero-3-phospho-1'-rac-glycerol) were purchased from Avanti Polar Lipids (Alabaster, AL, USA). 5NS (5-DOXYL-stearic acid) and 16NS (16-DOXIL-stearic acid) were purchased from Sigma. DMPC was chosen to mimic surface membrane of mammalian cells, as PC is the major component of mammalian cytoplasmic membranes, and because the lipid is stable to oxidation and readily hydrates in water forming lamellar phases at physiological pH and temperatures [19]. DMPG was chosen since phosphatidylglycerol is absent in

eukaryotic plasma membranes, but is ubiquitous and abundant in bacterial membranes [19] .

The working buffer was HEPES 10 mM pH 7.4 in NaCl 150 mM.

Surface pressure

Changes in the surface pressure of lipid monolayers induced by peptides 6 and 6.2 were measured in a Kibron Langmuir-Blodgett trough, at constant temperature (25 ± 0.5 °C). The surface of the buffer solution contained in a Teflon trough of fixed area was exhaustively cleaned by surface aspiration. Then, a chloroform solution of lipids was spread on this surface to reach surface pressures of 20.5 ± 1 mN/m. Peptide solutions were injected in the subphase and the changes of surface pressure were recorded until a constant value was reached.

Pressure data obtained were fitted with the follow equation:

$$\theta = \frac{\Delta\Pi}{\Delta\Pi_{\max}} = \frac{[peptide]^n}{k_d + [peptide]^n} \qquad (1)$$

Where θ corresponds to the degree of coverage, ΔΠ is the surface pressure shift, [peptide] is the peptide concentration, *n* is the heterogeneity parameter describing the width of energy distribution and k_d is the dissociation constant.

The adsorption rate constant (*k*) was calculated from the equation [20]:

$$\Delta\Pi = -e^{-kt}\Delta\Pi_{\max} + \Delta\Pi_{\max} \qquad (2)$$

The kinetics of peptides penetration was followed using:

$$\Delta\Pi = k^r \qquad (3)$$

from where the constants k and *r* [21] were determined.

Regression analyses of the ΔΠ vs. √time curves were performed to determine the values of *r*, with Graphpad Prism, by minimizing the root mean square error between the experimental data rate and the model equation.

Zeta potential

Zeta potential of liposomes was determined in a Z-meter 3.0 (Zeta Meter Inc, Staunton, VA, USA) by applying a continuous electric field of 50 V to a liposome suspension in buffer. The movement of the particle in the electrical field was followed by microscopic visualization in a reticulated objective. Values of the electrophoretic mobility (μ) were automatically given by the instrument. The zeta potential in volts (ξ) was calculated by the Smoluchowski equation:

$$\xi = 4\Pi \frac{\eta\mu}{D} \qquad (4)$$

where η is the viscosity of the suspension at 20 ºC, D is the dielectric constant of the solution at 20 ºC and μ is the electrophoretic mobility of particles (micrometer/sec per volt/cm)

Fluorescence spectroscopy measurements

Since peptides 6 and 6.2 contain tryptophan residues, fluorescence techniques are suitable tools for the analyses of these molecules. Fluorescence quenching studies were carried out in a Varian Cary Eclipse fluorescence spectrophotometer (Mulgrave, Australia). The fluorescence spectral characterization of peptides was performed at 290 nm to minimize the relative quencher/fluorophore light-absorption ratios. Fluorescence emission was collected at 350 nm (fixed wavelength). Excitation and emission spectra were corrected for wavelength-dependent instrumental factors [22, 23].

Acrylamide quenching

The fluorescence quenching of peptides (5 μM) by acrylamide was measured in buffer and in the presence of DMPC:DMPG (5:1) LUV (3 mM), by successive additions of small volumes of the quencher stock solution, ranging from 0 to 60 mM [24]. Each spectrum was recorded after 10 min incubation. Quenching data were analyzed using the Stern−Volmer equation [25]:

$$\frac{I_0}{I} = 1 + K_{SV} \cdot [Q] \qquad (5)$$

Where I and I_0 are the fluorescence intensities of the sample in the presence and absence of quencher respectively, K_{SV} is the Stern−Volmer constant and [Q] is the quencher concentration.

5NS and 16NS quenching

Fluorescence quenching assays with the lipophilic probes 5NS and 16NS were carried out at the same peptide and lipid concentrations used for the acrylamide quenching study. Briefly, by successive additions of small amounts of these quenchers in ethanol solution to the peptide samples in DMPC:DMPG (5:1), keeping the ethanol concentration below 2% (*v/v*) [26]. The effective lipophilic quencher concentration in the membrane was calculated from the partition coefficient of both quenchers to the lipid bilayers [27]. After each quencher addition, samples were incubated for 10 min before measurement. Quenching data were analyzed by using the Stern−Volmer equation (eq. 5), or the Lehrer equation (eq. 6) when a negative deviation from the Stern–Volmer relationship is observed. [27, 28]

$$\frac{I_0}{I} = \frac{1 + K_{SV}[Q]}{(1 + K_{SV}[Q])(1 - f_b) + f_b} \qquad (6)$$

where f_b corresponds to the fraction of light arising from the accessible fluorophores to

the quencher.

Circular dichroism in the far UV

We studied the secondary structure content by circular dichroism spectroscopy in the far UV, using a JASCO J-810 (Jasco Corp., Tokyo, Japan) spectropolarimeter, calibrated with (+)-10-camphorsulfonic acid. The measurements were performed under nitrogen gas flow of 8 l/h at a temperature of 20 °C, controlled by a Peltier system (JASCO). Spectra were recorded between 185 and 320 nm, using a 0.1 cm path-length cell. The peptide concentrations were 20 µM, dissolved in 10 mM sodium phosphate buffer pH 7.0, or the same buffer with sodium 10 mM dodecyl sulfate (SDS). The sensitivity was 100 millidegrees. We used a scan speed of 50 nm/min, a response time of 1 s and a bandwidth of 1 nm. We performed an average of five assays for each sample spectra. The average absorption was corrected by buffer and then baselined to zero using the average of readings between 290 and 320 nm. Finally, the data were smoothed using a Savizky-Golay fourth-degree polynomial, with a window of ten points. The spectra were converted to mean molar ellipticity residue using the relationship:

$$[\theta] = \frac{\theta}{10 \times c \times n \times d} \qquad (7)$$

where $[\theta]$ is the molar ellipticity (in degrees × cm^2 × $dmol^{-1}$), θ the ellipticity in millidegrees, n is the number of residues of the peptide and c its molar concentration, d is the length of the cell in centimeters.

The %AH (or alpha helical content) was calculated by following equation described in [29].

$$\%AH = \frac{(\theta_{222} + 2000) \times 100}{-30000} \qquad (8)$$

Membrane dipole potential assessed by di-8-ANEPPS

Human blood samples were obtained from healthy volunteers, with their previous written informed consent, at the Instituto Português do Sangue (Lisbon, Portugal). This study was approved by the ethics committee of the Faculdade de Medicina da Universidade de Lisboa. Isolation of erythrocytes and labeling of these cells with di-8-ANEPPS (Invitrogen, Carlsbad, CA, USA) were performed as described before [30] For erythrocytes isolation, blood samples were centrifuged at 1200 × *g* during 10 min, plasma and buffy-coat were removed, and remaining erythrocytes were washed twice in working buffer. They were incubated at 1% hematocrit in buffer supplemented with 0.05% (m/v) Pluronic F-127 (Sigma) and di-8-ANEPPS 10 µM. Cells were incubated with the fluorescent probe during 1 h, with gentle agitation, and the unbound probe was washed with Pluronic-free buffer on two centrifugation cycles. Peptide 6 and peptide 6.2 were incubated with erythrocytes at 0.02% hematocrit for 1 h, with gentle agitation, before the fluorescence measurements. Excitation spectra and the ratio of intensities at the excitation wavelengths of 455 and 525 nm ($R = I_{455}/I_{525}$) were obtained with emission set at 670 nm to avoid membrane fluidity-related artifacts. [31, 32] Excitation and emission slits for these measurements were set to 5 and 10 nm, respectively. The variation of R with the peptide concentration was analyzed by a single binding site model [33] :

$$\frac{R}{R_0} = 1 + \frac{\frac{R_{\min}}{R_0}[peptide]}{K_d + [peptide]} \qquad (9)$$

with the R values normalized for R_0, the value in the absence of peptide. $R_{\min}$ defines the asymptotic minimum value of R and K_d is the dissociation constant.

Results

Peptide design and determination of MIC, hemolytic activity and aggregation

Both peptides were designed from the previously reported antimicrobial peptide 2 (Seq2) [15]. Seq2 backbone was used as a scaffold to synthesize two new sequences suitable to study lipid selectivity in alpha-helical, amphipathic cationic peptides.

For peptide 6 (P6) we introduced the following substitutions to parental Seq2: we replaced K4 for W, L7 for G, K8 for W and K14 for L.

For peptide 6.2 (P6.2) we modified peptide 6 with the following substitutions: we replaced W4 for R, W8 for R, I16 for R and Y19 for K.

These specific substitutions made P6 to diminish its net charge (from 6 in Seq2 to 3) but retaining the isoelectric point (around 10 for both peptides). P6 also had an increased hydrophobicity but a diminished hydrophobic moment compared to Seq2.

Peptide 6.2 had an increased net charge and also an increased hydrophobic moment, but a diminished hydrophobicity compared to P6 (see table 1)

All these changes rendered two closely related peptides but with completely different activity toward biological membranes. Peptide 6 exhibited a high hemolytic activity and did not show significant antimicrobial activity against *P. aeuroginosas* or *S. aureus.* On the other hand, P6.2 showed a significant reduction of the hemolytic activity concomitant with a strong antimicrobial activity against both *P. aeuroginosas* and *S. aureus* (Table 1).

Finally, aggregation of the peptides in solution was evaluated ~~by~~ using the fluorescent probe 1-8-ANS that binds to hydrophobic portions of peptides and proteins and can be used to detect aggregation or changes in surface hydrophobicity [34]. As we can see in figure S1, peptide 6 had shown a slight blue shift of the emission maximum indicating some peptide aggregation ~~in~~ at the higher concentration tested. On the other hand, in the case of peptide 6.2 no significant changes were observed, in this case aggregation was probably prevented by the intercalation of charged residues among hydrophobic ones. This different behavior between the peptides was probably due to the higher number of charged residues that peptide 6.2 had, compared to peptide 6.

Membrane affinity

As was pointed above, the main objective of this work was to establish a correlation between membrane affinity and antimicrobial or hemolytic activity, in this regard, we chose two lipid formulations, pure DMPC as PC is mainly contained in mammalian membranes, and DMPC:DMPG 1:5 as a simplified model of bacterial membranes. In order to avoid misinterpretations, the concentration of peptides for these studies was kept below 5 µM, where no significant effects of aggregation were observed.

First, we evaluated the affinity of both peptides toward the model membranes described above by surface pressure assays.

As we can see in Figure 1, both peptides were able to induce changes in the surface pressure of pure DMPC membranes; however, P6 exhibited greater changes than P6.2. When interactions were quantified (assuming a Langmuir behavior by obtaining a dissociation constant (K_d)) we confirmed the higher affinity of P6 toward this membrane. This difference was reflected by the K_d value of P6, which was almost twice that of P6.2 (Table 2). On the other hand, when PG containing membranes were tested,

P6.2 exhibited a K_d four times lower than P6, indicating a higher affinity towards this kind of membranes (Figure 1b and Table 1).

In order to a better understanding of peptide-lipid interactions, a kinetic analysis was also performed. As we can see in Figure 1 and table 2, P6.2 exhibited a faster kinetics in PG containing monolayer, whereas P6 exhibited the fastest kinetics in pure PC monolayers. Finally, a relaxation coefficient (r) (defined according to Eq. 5) was obtained to characterize the peptide adsorption kinetics. In the case of P6.2, for all the conditions assayed, the r coefficient remained close to 0.5 (Table 2). On the other hand, the r coefficient obtained for P6 in PG containing membranes departs from 0.5, but on pure PC monolayers the behavior changed and the r coefficient remained close to 0.5 (Table 2).

It is well known that electrostatic forces play a key role in the interaction between peptides and the lipid membrane; in this context, in order to complement pressure information, we performed zeta potential experiments. Zeta potential is a surface property that represents an electrokinetic charge which occurs at the solid-liquid interface of particles.

As we can seen in Figure 2, zeta potential value for both types of liposomes becames more positive with the addition of peptides, as it expected due to the net positive charge of both peptides. These results confirmed an interaction between peptides and lipid membranes, in a good agreement with pressure data. Interestingly, when we compared

the behavior of both peptides with each lipid composition, we found a trend similar to that obtained earlier with monolayer experiments.

P6 exhibited a higher affinity with pure PC liposomes, while P6.2 showed a higher affinity with PG containing liposomes (Figure 2 and Table 1).

Finally, quenching experiments were conducted, Figure S2 (supplementary data) depicts Stern-Volmer curves obtained with three different quenchers used, Acrylamide, 5NS and 16NS. The fluorescence quenching for both peptides by acrylamide (a hydrophilic molecule) revealed that no hydrophobic pockets were present (linear Stern–Volmer plots; Fig. S2A). When the average position of Trp residues into the membrane was obtained, we found that Trp residues were buried 8.2 Å and 5.4 Å into the membrane, for P6.2 and P6 respectively. It should be pointed that, for each peptide, data represented the average position of all its Trps. The narrow half-width at half-height distributions obtained for P6.2 (1.32 Å) could be explained considering that the three Trps residues of the peptide are accommodated in a similar position into the membrane, indicating an arrangement parallel to the membrane, in good agreement with other CAMPs [35, 36]. In the case of P6 a widespread distribution (3.8 Å) was found, and that phenomenon could be related to a different distribution of Trps in the final secondary structure.

In order to validate our hypothesis, we obtain the helical wheel projection diagrams ~~by~~ for both peptides using *Heliquest* software (Figure S2). The wheel projections strongly suggested for P6.2 an alpha helix secondary structure leading a typical amphipathic structure found in many cationic antimicrobial peptides, with the three Trps residues in a similar plane. However, for P6 the amino acid constellation did not show a complete

amphipathic structure and the Trps seem to be in different planes, confirming our quenching data.

To experimentally determine the alpha-helix structure predicted for peptide 6.2, CD experiments in buffer and in the presence of SDS micelles were conducted (Figure S4). The spectra obtained confirmed an alpha-helix conversion in the presence of negatively charged micelles. Furthermore, if we plot the possible location of the alpha-helix structured peptide, as demonstrated by CD data, with the average location of Trp residues obtained by quenching assays, both results match perfectly (Figure 4).

Finally, after the characterization of the peptide interactions with the model membrane systems, we studied the interactions with red blood cells in order to complement the hemolytic data. For this purpose, we used isolated human erythrocytes labeled with the fluorescent probe di-8-ANEPPS, because in previous studies it proved to be a good reporter for the interaction of peptides with the plasma membranes of these cells [30, 37]. In these experiments, a suspension of probe-labeled erythrocytes was incubated 1 h with different peptide concentrations. The AMP-erythrocyte membrane interaction is followed by fluorescence, measuring the perturbations of the basal values of the dipole potential (i.e. value without peptide) that works as a reporter of the interaction.

The membrane dipole potential significantly decreased in the presence of P6, in contrast to P6.2, indicating a stronger interaction with the erythrocyte membrane. The latter also showed decreases in the dipole potential, but these changes were significantly lower

than the one obtained for P6 (Figure 5, Figure S4). These results are in good agreement with the hemolytic data listed in Table 1.

Discussion

The common subject in the mechanism for peptide antimicrobial activity is the interaction with membranes; and a general characteristic observed for AMPs is their ability to disturb bilayer integrity, concomitant with the collapse of the transmembrane electrochemical gradients [38, 39]. Several bilayer interactions and disruption models have been proposed for those AMPs that depend on membrane interference for their antimicrobial activity [40].

In order to get an insight into the possible factors involved in the type of lipid membrane selection by cationic AMPs, we designed two model peptides from a previously reported AMP (Seq2). These new sequences named P6 and P6.2 displayed very different activities on biological membranes. P6 was obtained after substituting 4 amino acids in the 19 residues sequence, we replace the two K at position 4 and 8 for two W at the same position (this shift from hydrophilic to hydrophobic residues produced a disruption in the hydrophilic face of the alpha helical structured peptide); we replaced the L at position 7 for G (a neutral small residue) and finally the K at position 14 was replaced for L. The result, as seen in figure S2, is a peptide (P6) with a continuous hydrophobic face, but with a disrupted hydrophilic face, this feature prevented the peptide from having antibacterial activity, but prompted it to have high hemolytic activity. For peptide 6.2 we simply turned it amphipathic by substituting the two hydrophobic W at positions 4 and 8 for two R respectively, the I at position 16 for R and Y19 for K. These changes rendered an amphipathic cationic AMP which in turn

became active against bacterial membranes and considerably diminished its hemolytic activity.

With these two model peptides, we decided to correlate the physicochemical features and the affinity toward different lipid composition membranes with antimicrobial and hemolytic activities. We chose two simple membrane models, one composed by pure DMPC (model of the mammalian member, as PC is the major component of the mammalian outer membrane) [41, 42], and a mix of DMPC:DMPG as a bacterial model membrane [19, 35, 36].

Our results from pressure data showed that P6.2 exhibited a higher affinity toward PG containing membranes, whereas P6 showed a higher affinity for pure PC membranes (Figure 1 and 2). Furthermore, the kinetics analysis also confirmed a faster kinetic of P6.2 toward PG containing membranes, whereas P6 exhibited a faster kinetic with pure PC monolayers. When the nature of the interaction was dissected, interestingly, we found that the higher and faster affinity of each peptide corresponds to a relaxation coefficient close to 0.5. When the *r* value is close to 0.5 the interactions could be described as Fickeans [43]. A physical interpretation of the relaxation coefficient (*r*) value can be discussed in terms of normal and anomalous diffusion of the peptides through the membrane. The linearity of the amount of substance adsorbed by a material with the square root of time assumes that the system responds to a linear gradient of concentration across the material in a steady state [44, 45]. In our context these results could be explained by the high and faster affinity of the peptides for each kind of membrane, the ligand (in our case the membrane) it is not able to respond to the perturbation, resulting finally in the disruptive effect that leads to bacterial death (in the case of P6.2) or the hemolysis (for P6).

Considering that DMPG and DMPC bilayers share the same basic features (cylindrical shape, chain tilt and thermodynamic behavior) and that the only marked difference is the charge of the head group of the phospholipids [42], zeta potential measures were conducted. Interestingly, besides the change in the model system from a lipid air/water monolayer to a bilayer (by using liposomes) the same behavior was observed. Peptide 6.2 exhibited a 3.5 fold lower K_d value than peptide 6 on PG containing membranes, but when pure PC membranes were tested, K_d value of this peptide was 3 fold higher.

Up to this point, we were able to correlate the high hydrophobicity of P6 with an increased affinity towards zwitterionic membranes which could explain its hemolytic activity. In order to get a deeper insight in the relation between membrane affinity and hemolysis, we conducted di-8-ANNEPs experiments that allowed us to specifically evaluate the affinity of each peptide for erythrocyte membrane. The results showed in Figure 5 indicate a strong correlation between membrane affinity and hemolytic activity, confirming that the main reason of hemolytic activity in P6 is related to the ability of this molecule to bind the erythrocyte membrane. Furthermore, at least for this set of peptides, we are able to conclude that the main factor that drives the hemolysis is related to the affinity of the peptides toward the erythrocyte membrane. These data are in good agreement with our previous publication with related peptides [35], where peptide 8 that displayed a higher affinity towards pure PC membranes also correlated with increased erythrocytes membrane affinity, leading to higher hemolytic activity.

Finally, in order to confirm if the high affinity of P6.2 toward PG containing membranes could be associated with its high hydrophobic moment, fluorescent quenching and CD studies were conducted. This phenomenon, that allows the peptide to adopt an α-helix structure in contact with the membrane, would also increases its ability to interact with negatively charged membranes.

The Trp position data together with helical wheel projection and CD results confirmed us that peptide 6.2 binds to the membrane through a process governed by electrostatic forces, followed by an alpha-helix conversion. This characteristic allows the insertion of all Trp residues in a similar plane, in the carbon-chain region, stabilizing the interaction by an initial parallel alignment of the peptide in the membrane, in good agreement with previous reports for related AMPs [35]; and finally when accumulation of peptides becomes critical, the antimicrobial activity it is triggered. The lower affinity of P6 towards PG containing membranes in addition to its inability to adopt an amphipathic structure seems to be the main reason that explains the absence of antimicrobial activity in the conditions tested.

Overall, our data allow us to conclude that the selectivity of the peptides for zwitterionic or negatively charged lipids determine its bioactivity; in other words, affinity towards negatively charged lipids instead of zwitterionic ones, seems to be a key factor that drives from hemolytic to antimicrobial results.

ACKNOWLEDGEMENT

This work was supported by grants from Universidad Nacional de Quilmes, Comisión de Investigaciones Científicas de la Provincia de Buenos Aires (CIC-BA), Agencia Nacional de Promocion Cientıfica y Tecnologica (ANPCyT– MINCyT), PICT 2013-1481, PICT 2013-815, CONICET, Argentina; PIP-2014-11220130100383CO and Fundação para a Ciência e Tecnologia – Ministério da Educação e Ciência (FCT-MEC, Portugal). LS is a member of the Research Career of CIC-BA. AH, EAD and PCM are members of the Carrera del Investigador Cientıfico y Tecnologico (CONICET, Argentina). MM. and MEN acknowledge fellowships from CONICET, PM has a fellowship from CIN (Consejo Interuniversitario Nacional, Argentina).

References

[1] I.A. Edwards, A.G. Elliott, A.M. Kavanagh, J. Zuegg, M.A.T. Blaskovich, M.A. Cooper, Contribution of Amphipathicity and Hydrophobicity to the Antimicrobial Activity and Cytotoxicity of β-Hairpin Peptides, ACS Infectious Diseases, (2016).
[2] E. Gazit, I.R. Miller, P.C. Biggin, M.S. Sansom, Y. Shai, Structure and orientation of the mammalian antibacterial peptide cecropin P1 within phospholipid membranes, Journal of molecular biology, 258 (1996) 860-870.
[3] Y. Shai, Mode of action of membrane active antimicrobial peptides, Peptide Science, 66 (2002) 236-248.
[4] K.A. Brogden, Antimicrobial peptides: pore formers or metabolic inhibitors in bacteria?, Nature reviews. Microbiology, 3 (2005) 238-250.
[5] M. Avila, N. Said, D.M. Ojcius, The book reopened on infectious diseases, Microbes and infection / Institut Pasteur, 10 (2008) 942-947.
[6] R.E.W. Hancock, D.S. Chapple, Peptide antibiotics, Antimicrobial Agents and Chemotherapy, 43 (1999) 1317-1323.
[7] L. Zhang, A. Rozek, R.E.W. Hancock, Interaction of Cationic Antimicrobial Peptides with Model Membranes, Journal of Biological Chemistry, 276 (2001) 35714-35722.
[8] M.R. Yeaman, N.Y. Yount, Mechanisms of antimicrobial peptide action and resistance, Pharmacological reviews, 55 (2003) 27-55.
[9] M.N. Melo, R. Ferre, M.A. Castanho, Antimicrobial peptides: linking partition, activity and high membrane-bound concentrations, Nature reviews. Microbiology, 7 (2009) 245-250.
[10] Z. Jiang, A.I. Vasil, J.D. Hale, R.E. Hancock, M.L. Vasil, R.S. Hodges, Effects of net charge and the number of positively charged residues on the biological activity of amphipathic alpha-helical cationic antimicrobial peptides, Biopolymers, 90 (2008) 369-383.
[11] M. Dathe, H. Nikolenko, J. Meyer, M. Beyermann, M. Bienert, Optimization of the antimicrobial activity of magainin peptides by modification of charge, FEBS Lett, 501 (2001) 146-150.
[12] I. Zelezetsky, A. Tossi, Alpha-helical antimicrobial peptides--using a sequence template to guide structure-activity relationship studies, Biochim Biophys Acta, 9 (2006) 18.
[13] M.M. Domingues, R.G. Inacio, J.M. Raimundo, M. Martins, M.A. Castanho, N.C. Santos, Biophysical characterization of polymyxin B interaction with LPS aggregates and membrane model systems, Biopolymers, 98 (2012) 338-344.
[14] M.N. Melo, M.A. Castanho, The Mechanism of Action of Antimicrobial Peptides: Lipid Vesicles vs. Bacteria, Frontiers in immunology, 3 (2012) 236.
[15] D. Faccone, O. Veliz, A. Corso, M. Noguera, M. Martinez, C. Payes, L. Semorile, P.C. Maffia, Antimicrobial activity of de novo designed cationic peptides against multi-resistant clinical isolates, European journal of medicinal chemistry, 71 (2014) 31-35.
[16] R. Gautier, D. Douguet, B. Antonny, G. Drin, HELIQUEST: a web server to screen sequences with specific alpha-helical properties, Bioinformatics, 24 (2008) 2101-2102.
[17] E. Lacroix, A.R. Viguera, L. Serrano, Elucidating the folding problem of alpha-helices: local motifs, long-range electrostatics, ionic-strength dependence and prediction of NMR parameters, Journal of molecular biology, 284 (1998) 173-191.
[18] Pure Appl. Chem, 79 (2007) 717-728.

[19] T. Shireen, A. Basu, M. Sarkar, K. Mukhopadhyay, Lipid composition is an important determinant of antimicrobial activity of alpha-melanocyte stimulating hormone, Biophysical chemistry, 196 (2015) 33-39.
[20] D. Jiang, K.L. Dinh, T.C. Ruthenburg, Y. Zhang, L. Su, D.P. Land, F. Zhou, A kinetic model for beta-amyloid adsorption at the air/solution interface and its implication to the beta-amyloid aggregation process, The journal of physical chemistry. B, 113 (2009) 3160-3168.
[21] J. Crank, The mathematics of diffusion, Oxford University Press, Oxford, 1975.
[22] M. Kubista, R. Sjoback, S. Eriksson, B. Albinsson, Experimental correction for the inner-filter effect in fluorescence spectra, Analyst, 119 (1994) 417-419.
[23] A.S. Ladokhin, S. Jayasinghe, S.H. White, How to measure and analyze tryptophan fluorescence in membranes properly, and why bother?, Analytical biochemistry, 285 (2000) 235-245.
[24] H.G. Franquelim, L.M. Loura, N.C. Santos, M.A. Castanho, Sifuvirtide screens rigid membrane surfaces. establishment of a correlation between efficacy and membrane domain selectivity among HIV fusion inhibitor peptides, J Am Chem Soc, 130 (2008) 6215-6223.
[25] N.C. Santos, M. Castanho, Fluorescence spectroscopy methodologies on the study of proteins and peptides. On the 150th anniversary of protein fluorescence, Trends Appl. Spectrosc., 4 (2002) 113-125.
[26] M. Yamazaki, M. Miyazu, T. Asano, A. Yuba, N. Kume, Direct evidence of induction of interdigitated gel structure in large unilamellar vesicles of dipalmitoylphosphatidylcholine by ethanol: studies by excimer method and high-resolution electron cryomicroscopy, Biophys J, 66 (1994) 729-733.
[27] N.C. Santos, M. Prieto, M.A.R.B. Castanho, Interaction of the major epitope region of HIV protein gp41 with membrane model systems. A fluorescence spectroscopy study, Biochemistry, 37 (1998) 8674-8682.
[28] J.F. Nagle, M.C. Wiener, Structure of fully hydrated bilayer dispersions, Biochim Biophys Acta, 942 (1988) 1-10.
[29] S.-H. Lee, S.-J. Kim, Y.-S. Lee, M.-D. Song, I.-H. Kim, H.-S. Won, De novo generation of short antimicrobial peptides with simple amino acid composition, Regulatory Peptides, 166 (2011) 36-41.
[30] P.M. Matos, M.A.R.B. Castanho, N.C. Santos, HIV-1 fusion inhibitor peptides enfuvirtide and T-1249 interact with erythrocyte and lymphocyte membranes, PloS one, 5 (2010) e9830.
[31] E. Gross, R.S. Bedlack, Jr., L.M. Loew, Dual-wavelength ratiometric fluorescence measurement of the membrane dipole potential, Biophys J, 67 (1994) 208-216.
[32] R.J. Clarke, D.J. Kane, Optical detection of membrane dipole potential: avoidance of fluidity and dye-induced effects, Biochimica et biophysica acta, 1323 (1997) 223-239.
[33] J. Cladera, P. O'Shea, Intramembrane molecular dipoles affect the membrane insertion and folding of a model amphiphilic peptide, Biophys J, 74 (1998) 2434-2442.
[34] A. Hawe, M. Sutter, W. Jiskoot, Extrinsic fluorescent dyes as tools for protein characterization, Pharmaceutical research, 25 (2008) 1487-1499.
[35] A. Hollmann, M. Martinez, M.E. Noguera, M.T. Augusto, A. Disalvo, N.C. Santos, L. Semorile, P.C. Maffia, Role of amphipathicity and hydrophobicity in the balance between hemolysis and peptide-membrane interactions of three related antimicrobial peptides, Colloids and surfaces. B, Biointerfaces, 141 (2016) 528-536.
[36] A.M. Bouchet, N.B. Iannucci, M.B. Pastrian, O. Cascone, N.C. Santos, E.A. Disalvo, A. Hollmann, Biological activity of antibacterial peptides matches synergism

between electrostatic and non electrostatic forces, Colloids and surfaces. B, Biointerfaces, 114 (2014) 363-371.
[37] F. Vigant, A. Hollmann, J. Lee, N.C. Santos, A.N. Freiberg, M.E. Jung, B. Lee, The Rigid Amphipathic Fusion Inhibitor dUY11 Acts Through Photosensitization of Viruses., J Virol, (2013).
[38] Y. Shai, Mechanism of the binding, insertion and destabilization of phospholipid bilayer membranes by α-helical antimicrobial and cell non-selective membrane-lytic peptides, Biochimica et Biophysica Acta (BBA)-Biomembranes, 1462 (1999) 55-70.
[39] B. Bechinger, Insights into the mechanisms of action of host defence peptides from biophysical and structural investigations, Journal of Peptide Science, 17 (2011) 306-314.
[40] G.G. Perron, M. Zasloff, G. Bell, Experimental evolution of resistance to an antimicrobial peptide, Proceedings of the Royal Society of London B: Biological Sciences, 273 (2006) 251-256.
[41] Z. Sojcic, H. Toplak, R. Zuehlke, U.E. Honegger, R. Buhlmann, U.N. Wiesmann, Cultured human skin fibroblasts modify their plasma membrane lipid composition and fluidity according to growth temperature suggesting homeoviscous adaptation at hypothermic (30 degrees C) but not at hyperthermic (40 degrees C) temperatures, Biochim Biophys Acta, 17 (1992) 31-37.
[42] N. Malanovic, R. Leber, M. Schmuck, M. Kriechbaum, R.A. Cordfunke, J.W. Drijfhout, A. de Breij, P.H. Nibbering, D. Kolb, K. Lohner, Phospholipid-driven differences determine the action of the synthetic antimicrobial peptide OP-145 on Gram-positive bacterial and mammalian membrane model systems, Biochimica et Biophysica Acta (BBA) - Biomembranes, 1848 (2015) 2437-2447.
[43] A. Hollmann, L. Delfederico, G. De Antoni, L. Semorile, E.A. Disalvo, Relaxation processes in the adsorption of surface layer proteins to lipid membranes, The journal of physical chemistry. B, 114 (2010) 16618-16624.
[44] M.F. Martini, E.A. Disalvo, Superficially active water in lipid membranes and its influence on the interaction of an aqueous soluble protease, Biochimica et Biophysica Acta (BBA) - Biomembranes, 1768 (2007) 2541-2548.
[45] H. Sanabria, Y. Kubota, M.N. Waxham, Multiple Diffusion Mechanisms Due to Nanostructuring in Crowded Environments, Biophysical Journal, 92 (2007) 313-322.

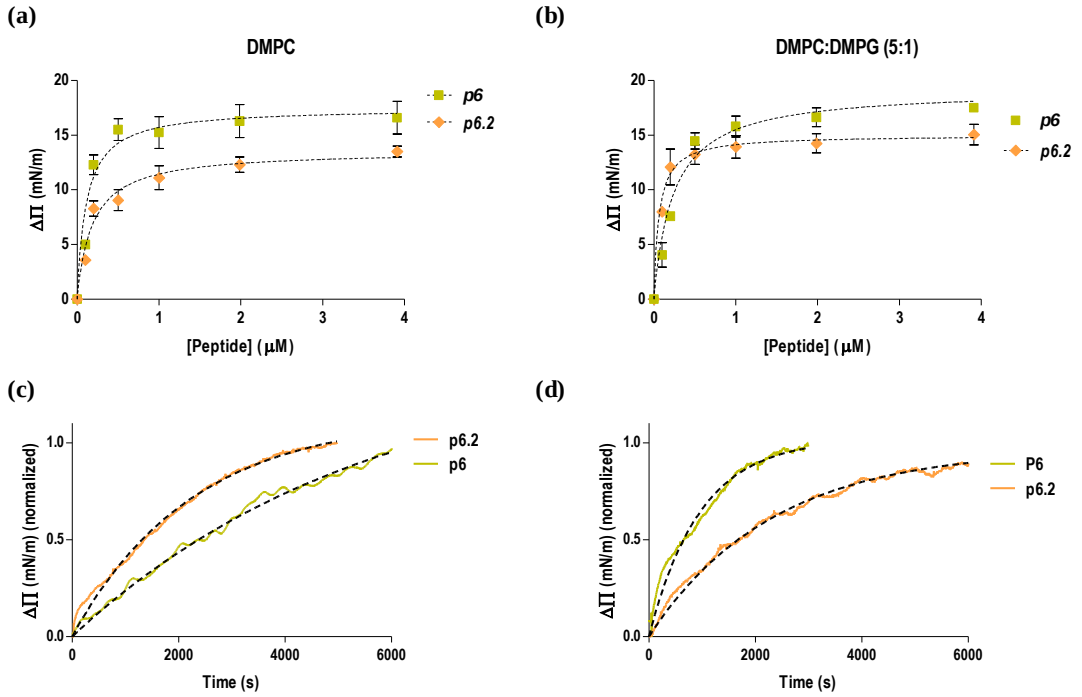

Figure 1. Interaction of peptides with lipid monolayers. Changes in the surface pressure expressed as ΔΠ as a function of the peptide concentration on pure DMPC monolayers (A) or DMPC:DMPG (5:1) monolayers (B). Changes in the surface pressure expressed as ΔΠ as a function of time after addition of each peptide to reach a final concentration of 0.2 μM on pure DMPC monolayers (C) or DMPC:DMPG (5:1) monolayers (D). The initial pressure was 21 ± 1 mN/m for all assays. Values are presented as mean ± standard deviation (SD); n=3.

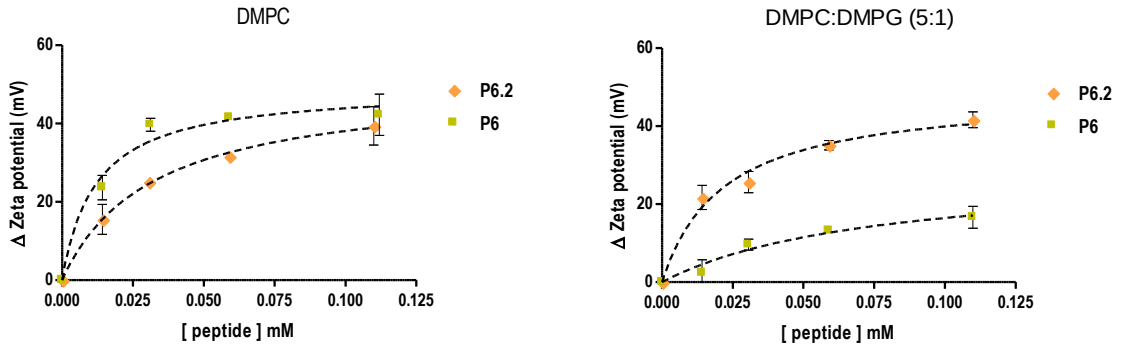

Figure 2. Zeta potential values of liposomes composed of pure DMPC (A) or DMPC:DMPG (5:1) (B) incubated with different amounts of peptides. Each point represents the averages of twenty independent measurements in at least three different batches. Error bars indicate standard deviations of the means.

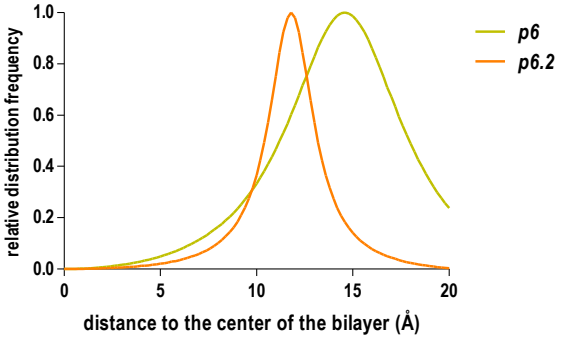

Figure 3. Localization of the peptides in the bilayer. In-depth localization of Trps residues of both peptides inside the membrane using the SIMEXDA method.

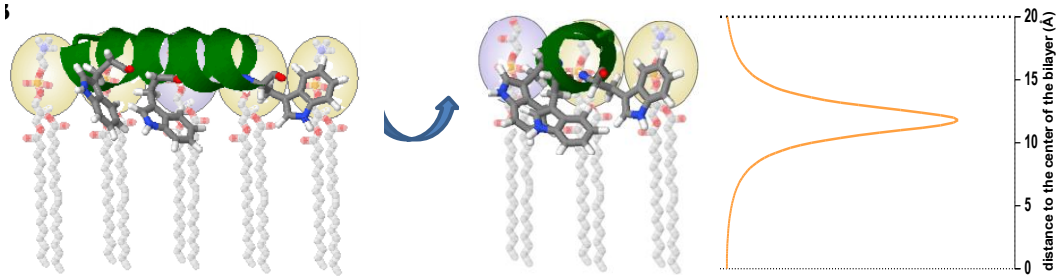

Figure 4. Cartoon representation of peptides 6.2 with the Trp residues represented as sticks using *Jmol* software (Jmol v. 14.2.9_2014.11.17) with the lipid monolayer as background (left graphic). In-depth localization of Trp residues of peptide 6.2 (right plot).

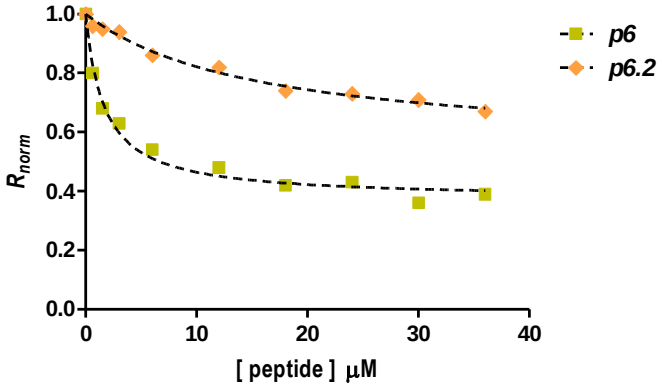

Figure 5. Antimicrobial peptide interactions with red blood cells. Binding profiles of peptides to erythrocyte cell membranes is depicted by plotting the di-8-ANEPPS excitation ratio, R (I_{455}/I_{525}, normalized to the initial value), as a function of the peptide concentration (C).

Table 1. Physicochemical parameters and biological activity of the two peptides and the parental peptide 2 (Seq2). MW: molecular weight; IP: isoelectric point; NC: net charge; μH: hydrophobic moment; H: hydrophobicity. MIC: minimal inhibitory concentration. The % hemolysis was obtained at 128 μg/ml for each peptide.

Peptide	Physicochemical parameters					MIC (μg/ml)		% Hemolysis
	MW*	IP*	NC**	μH**	H**	*P. aeruginosa*	*S. aureus*	
Peptide 2	**2421.02**	**10.39**	**6**	**0.622**	**0.409**	**64**	**32**	**30.47**
Peptido 6	**2465.97**	**10**	**3**	**0.363**	**0.803**	**>1024**	**>1024**	**51.36**
Peptido 6.2	**2515.09**	**11.75**	**7**	**0.793**	**0.328**	**32**	**32**	**34.46**

* Data obtained from http://web.expasy.org/compute_pi/
** Data obtained from http://heliquest.ipmc.cnrs.fr/cgi-bin/ComputParamsV2.py

Table 2. Apparent dissociation constants, $K_{d\ (pressure)}$ or $K_{d\ (P.\ zeta)}$, $\Delta\Pi_{max,}$ k and r determined from surface pressure experiments or zeta potential obtained by fitting data using Eq. 1, 2 y 3 respectively. Values are presented as mean ± standard deviation (SD).

Lipid	Peptide	K_d *(Pressure)*	ΔΠmax	$k \times 10^{-3}$	r	K_d *(P. zeta)*
DMPC	**P6**	**0,11 ± 0.03**	**17.9 ± 1.2**	**1.036 ± 0.011**	**0.463 ± 0.003**	**0.012 ± 0.004**
	P6.2	**0,18 ± 0.04**	**12.9 ± 0.8**	**0.204 ± 0.001**	**0.417 ± 0.001**	**0.032 ± 0.002**
DMºPC:DMPG	**P6**	**0.24 ± 0.04**	**17.3 ± 1.0**	**0.146 ± 0.001**	**0.737 ± 0.002**	**0.080 ± 0.030**
	P6.2	**0.06 ± 0.02**	**15.0 ± 0.6**	**0.443 ± 0.003**	**0.566 ± 0.002**	**0.021 ± 0.005**